Cross-section and couplings measurements with the ATLAS detector for the 125 GeV Higgs boson in the diboson decay channels

William Leight, on behalf of the ATLAS Collaboration

DESY

E-mail: william.leight@desy.de

Detailed measurements of the properties of the 125 GeV Higgs boson are fundamental for the understanding of the electroweak symmetry breaking mechanism. Measurements of the Higgs boson in the diboson final states allow to study the gauge and loop induced couplings of the Higgs boson both in production and decay. This talk summarizes ATLAS measurements of the 125 GeV Higgs boson in decays involving W, Z bosons or photons.

XXV International Workshop on Deep-Inelastic Scattering and Related Subjects
3-7 April 2017
University of Birmingham, UK

1. Introduction

The ATLAS detector at the LHC is a multi-purpose particle detector with excellent detection and reconstruction capabilities [1]. During the LHC Run-1, the ATLAS and CMS collaborations discovered a new particle with a mass of approximately 125 GeV [2, 3]. During Run-1 and the first years of Run-2, numerous further measurements of this particle were carried out, all of which have been compatible with the hypothesis that this particle is the Standard Model (SM) Higgs boson. Detailed and precise measurements of its properties, in particular couplings to other particles, are obviously essential for further understanding of electroweak symmetry breaking. These can be obtained by probing different production mechanisms: at the LHC, the dominant Higgs boson production mechanisms is gluon-gluon fusion (ggH), in which the Higgs boson is produced via a heavy (usually top) quark loop, but production from vector boson fusion (VBF), in association with a vector boson (VH), with a $t\bar{t}$ or $b\bar{b}$ pair ($t\bar{t}H/b\bar{b}H$), or with a single top (tH) can also in principle be identified by looking at the particles accompanying the Higgs boson decay products. Diboson decay channels provide relatively clean signals that can be used for such measurements. Below, an overview is given of recent ATLAS results from decays of the Higgs boson to pairs of photons or W or Z bosons.

2. Results in the $H \rightarrow ZZ^* \rightarrow 4\ell$ Decay Channel

The $H \rightarrow ZZ^* \rightarrow 4\ell$ decay channel features a high signal to background ratio of about 2 in the 4ℓ invariant mass window around the Higgs boson peak, as can be seen in Figure 1: however, because both Z bosons are required to decay to a pair of electrons or muons the overall branching ratio is only about 0.013%, which is further reduced by an acceptance×efficiency of 16-31% depending on the final state (muon reconstruction being more efficient than electron reconstruction in ATLAS). To enhance the statistics, loose particle ID and isolation selections are applied; to improve the resolution, the mass of the leading lepton pair (and its FSR photons) is kinematically constrained to the mass of the Z boson. Several refinements to the analysis were made in Run-2: the new Inner B-layer, a pixel detector layer close to the beamline, provides additional rejection of electron backgrounds, the muon p_T selection was lowered from 6 GeV to 5 GeV to provide an additional 8% acceptance, and a 4ℓ vertexing constraint was added to the event selection to reject additional background. The dominant background is from non-resonant SM ZZ^* production and is estimated from simulation, while smaller backgrounds from Z+jets and $t\bar{t}$ are measured using data-driven methods. This section reports cross-section and production mode measurements in this decay channel using 14.8 fb^{-1} of $\sqrt{s} = 13$ TeV data collected in 2015-2016 [4].

Both fiducial and total cross-sections are measured. The fiducial cross-section, defined as $\sigma^{fid} = N_S/(C \times \mathcal{L})$, where N_S is the number of signal events, $\mathcal{L}$ is the integrated luminosity, and C corrects for detector efficiency and resolution, is the more model-independent measurement, as it is free of assumptions about acceptance or branching ratio. Cross-sections are measured for each final state independently: the final result is obtained from a likelihood fit to the $m_{4\ell}$ distribution for the given final state (or all final states) in the range 115<$m_{4\ell}$<130 GeV (assuming $m_H = 125.09$ GeV). A comparison of the measured fiducial cross-sections and the SM prediction is given in Table 1. A total cross-section is then obtained by assuming SM values of the acceptance and
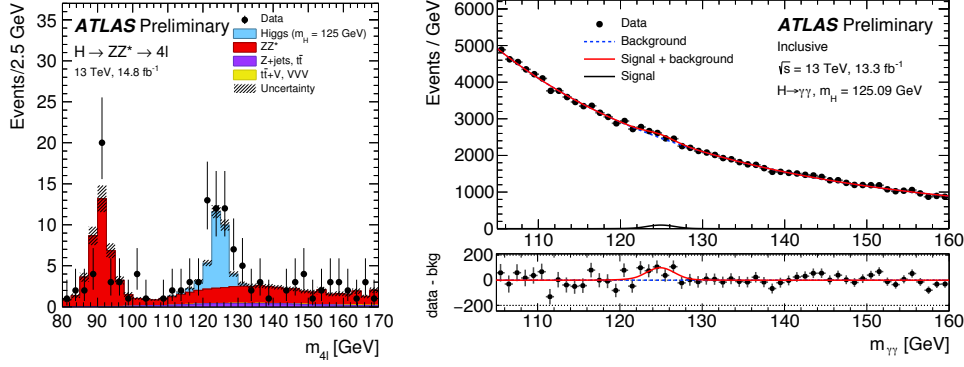
Figure 1: Left, Data-MC comparison of the $m_{4\ell}$ distribution after analysis selections[4]. Right, the $m_{\gamma\gamma}$ distribution after analysis selections, with the data-background shown in the lower panel [5].

branching ratio. The result is $\sigma_{tot} = 81^{+18}_{-16}$ pb, compatible with the SM prediction of $\sigma_{tot,SM} = 55.5^{+3.8}_{-4.4}$ pb at 1.6σ. The uncertainties here are still statistically dominated.

Table 1: Measured and predicted fiducial cross-sections for each 4ℓ final state [4].

Final state	measured σ_{fid} [fb]	$\sigma_{\text{fid, SM}}$ [fb]
4μ	$1.28^{+0.48}_{-0.40}$	$0.93^{+0.06}_{-0.08}$
$4e$	$0.81^{+0.51}_{-0.38}$	$0.73^{+0.05}_{-0.06}$
$2\mu2e$	$1.29^{+0.58}_{-0.46}$	$0.67^{+0.04}_{-0.04}$
$2e2\mu$	$1.10^{+0.49}_{-0.40}$	$0.76^{+0.05}_{-0.06}$

To probe the couplings, events in the 118<$m_{4\ell}$<129 GeV range are sorted into five exclusive categories. The VH-leptonic category requires one additional lepton with p_T of at least 8 GeV; if no such lepton is present, the event is sorted by the number of jets (which must have $p_T >$ 30 GeV), with the 2-jet category further broken down into VH-like or VBF-like for m_{jj} less than or greater than 120 GeV. In all categories except VH-leptonic, a Boosted Decision Tree (BDT) is used to further enhance the sensitivity, and the signal is obtained from a likelihood fit to the BDT output. Cross-section × branching ratio values are then calculated assuming $m_H = 125.09$ GeV. Measurements are obtained in the ggH (combined with $t\bar{t}H$, tH, and $b\bar{b}H$ as there is no sensitivity to them yet) and VBF modes (only a limit can be set on VH), compatible with the SM production at less than 1.5σ in both cases, as can be seen in Table 2.

Table 2: Measured and predicted production mode $\sigma \times$ BF for the 4ℓ final state [4].

$\sigma \times$ BF	Measurement [pb]	SM prediction [pb]
$\sigma_{\text{ggH}+b\bar{b}H+t\bar{t}H} \cdot \mathscr{B}(H \to ZZ^*)$	$1.80^{+0.49}_{-0.44}$	1.31 ± 0.07
$\sigma_{\text{VBF}} \cdot \mathscr{B}(H \to ZZ^*)$	$0.37^{+0.28}_{-0.21}$	0.100 ± 0.003
$\sigma_{VH} \cdot \mathscr{B}(H \to ZZ^*)$	$0^{+0.15}$	0.059 ± 0.002

3. Results in the $H \rightarrow \gamma\gamma$ Decay Channel

The $H \rightarrow \gamma\gamma$ decay channel is still relatively clean while not being as statistics-limited as the 4ℓ channel thanks to a branching ratio that is an order of magnitude larger. To remove background, tight ID and isolation requirements are imposed on the photons. The mass of the photon pair is calculated using a vertex found by a neural network. The resulting Higgs boson mass peak sits on top of a smoothly falling $m_{\gamma\gamma}$ distribution from the diphoton background, as seen in Figure 1. This background consists mainly of SM diphoton processes, plus contributions from jets misidentified as photons. To extract the signal, analytical models are constructed for both the signal and the background, and a signal+background fit is performed to the $m_{\gamma\gamma}$ distribution. The background model is chosen to minimize the amount of signal measured when the signal+background fit is performed on a background-only simulation. This section reports cross-section and production mode measurements in this decay channel using 13.3 fb^{-1} of $\sqrt{s} = 13$ TeV data collected in 2015-2016, as well as results obtained by combining measurements from this and the 4ℓ channel [5, 6].

As with the 4ℓ channel, the total cross-section is extracted using bin-by-bin correction factors and assuming $m_H = 125.09$ GeV. The result, $\sigma_{fid} = 43.2 \pm 14.9(\text{stat}) \pm 4.9(\text{syst})$ fb, agrees reasonably well with the SM prediction of $\sigma_{fid,SM} = 62.8^{+3.4}_{-4.4}$ fb. Additionally, the higher statistics of the $\gamma\gamma$ decay channel allow measuring differential cross-sections, which are obtained for the variables $p_T^{\gamma\gamma}$ (shown in Figure 2), $|y_{\gamma\gamma}|$, N_{jets} (both inclusive, as shown in Figure 2, and exclusive), m_{jj}, $p_{T,j1}$, $|cos(\theta^*)|$, and $\Delta\phi_{jj}$. These measurements are compared to various theoretical predictions, with no significant disagreements with the SM observed. It is also possible to measure simplified template cross-sections (STXS) in the $\gamma\gamma$ channel at the simplest level, stage 0. The STXS framework provides a series of exclusive phase-space regions that can be measured by all decay channels (though not all channels are sensitive in all regions), in order to minimize theory dependence by separating between production modes [7]. In order to measure the STXS stage 0 cross-sections, the events are sorted into 13 exclusive categories, each enriched in different production modes and with different signal/background ratios, and a simultaneous fit is performed to the $m_{\gamma\gamma}$ distribution in each category. The results are given in Table 3: all agree with the SM within 1-2σ.

Table 3: STXS stage 0 results($\times$ branching ratio) for the $\gamma\gamma$ final state [5].

$\sigma \times \text{BF}$	Measurement [fb]
$\sigma_{ggH} \times \mathscr{B}(H \rightarrow \gamma\gamma)$	63^{+30}_{-29}
$\sigma_{\text{VBF}} \times \mathscr{B}(H \rightarrow \gamma\gamma)$	$17.8^{+6.3}_{-5.7}$
$\sigma_{\text{VHlep}} \times \mathscr{B}(H \rightarrow \gamma\gamma)$	$1.0^{+2.5}_{-1.9}$
$\sigma_{\text{VHhad}} \times \mathscr{B}(H \rightarrow \gamma\gamma)$	$-2.3^{+6.8}_{-5.8}$
$\sigma_{t\bar{t}H} \times \mathscr{B}(H \rightarrow \gamma\gamma)$	$-0.3^{+1.4}_{-1.1}$

Further sensitivity can be obtained by combining results from the $\gamma\gamma$ and 4ℓ channels. Assuming SM acceptance and branching ratios, a total cross-section is obtained that agrees well with theoretical predictions, as shown in Figure 3. Additionally, improvements in the $\sigma \times \mathscr{B}$ measurements can be obtained from a likelihood fit that treats each production mode $\times$ branching ratio cross-section as independent, where the production modes are ggH (which includes $b\bar{b}$H due to lack of statistics, with the SM-predicted ratio of the two processes used to combine them), VBF,
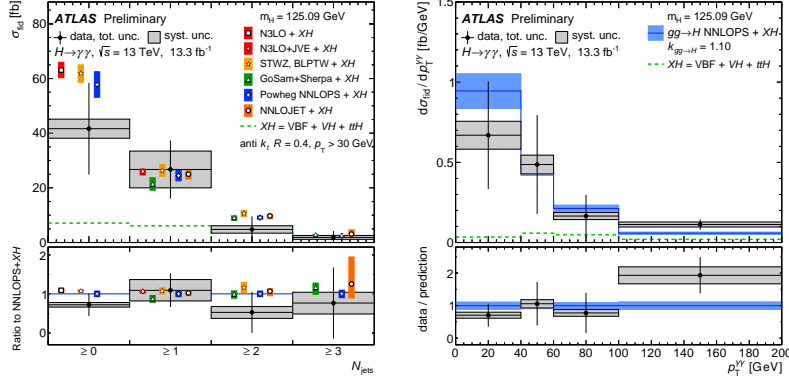
Figure 2: Differential cross-sections in the $\gamma\gamma$ decay channel: left, for inclusive N_{jets}, compared to several theory calculations of ggH production (plus predictions for VBF, VH, and $t\bar{t}H$); right, for $p_T^{\gamma\gamma}$ [5].

VHlep and VHhad ("lep" and "had" indicate the V boson decay; WH and ZH are also combined using their SM-predicted ratio) and top (a combination of $t\bar{t}H$ and tH, again using their SM-predicted ratio). [In the case of ZZ^* decay and VH or $t\bar{t}H$, where there is no constraint from data, the $\sigma \times \mathscr{B}$ value is fixed to the SM prediction.] Although the results are obtained in the separate decay channels, the combined likelihood fit allows for numerous systematic uncertainties, both experimental and theoretical, to be correlated between them, producing a more precise result. In all cases, the results, shown in Figure 3, are compatible with the SM prediction.
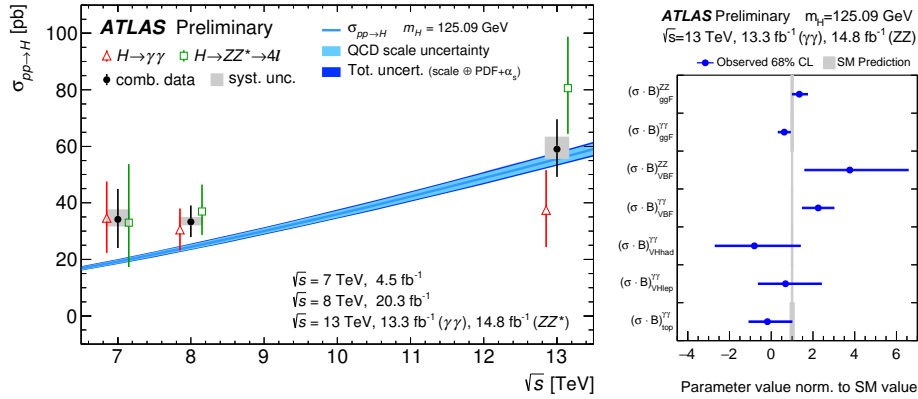

Figure 3: Left, total Higgs boson production cross-section vs. $\sqrt{s}$, for the 4ℓ and $\gamma\gamma$ channels separately and combined. Right, $\sigma \times \mathscr{B}$ values obtained from the independent fit described in the text. [6]

4. Results in the $H \rightarrow WW^* \rightarrow \ell\nu\ell\nu$ Decay Channel

Even with the requirement that both W bosons decay leptonically, this channel has a branching ratio of about 1%, higher than either of the previous channels. However, it has many backgrounds – SM top processes, V+jets, SM WW and other VV processes, $Z \rightarrow \tau\tau$, etc. – and a non-fully-reconstructed final state, making for a challenging analysis. Since background suppression is essential, tight lepton ID and isolation selections are imposed. Drell/Yan background processes are

further suppressed by requiring an eμ final state; top quark processes are removed by vetoing b-jets. Further background rejection can be obtained by using the extra jet or lepton signatures from production modes other than ggH (though this does have some cost in statistics, and also introduces ggH production as an additional background). The results described here are for the VBF and WH production modes, using 5.8 fb^{-1} of $\sqrt{s} = 13$ TeV data collected in 2015-2016 [8].

The VBF and WH production categories are constructed to be orthogonal. The VBF category requires 2 jets in addition to the eμ pair, but a third lepton is vetoed. Both leptons must lie between the two jets, which must have no additional jet between them. Additionally, $Z \to \tau\tau$ decays are explicitly vetoed. The WH category, on the other hand, requires exactly 3 leptons (with a total charge of ± 1) and at most one jet, with a Z boson veto and a requirement of at least 50 GeV of missing transverse energy. Further, the closest eμ pair must have $\Delta R < 0.2$. For each category, several control regions, each enriched in a leading background, are constructed, and the signal is obtained from a simultaneous fit to the signal and control region yields. For the VBF production mode, a BDT is used to improve the result, with the signal region split in two based on the BDT score. The resulting signal strengths are $\mu_{\text{VBF}} = 1.7^{+1.0}_{-0.8}(\text{stat})^{+0.6}_{-0.4}(\text{syst})$ and $\mu_{WH} = 3.2^{+3.7}_{-3.2}(\text{stat})^{+2.3}_{-2.7}(\text{syst})$, providing agreement with the SM within uncertainties that are still quite large.

5. Summary and Outlook

Thanks to their relatively clean signatures, diboson decay channels continue to provide an important probe of Higgs boson properties. So far, no significant deviations from the SM predictions have been observed. However, the analyses presented above cover only a portion of the full 2015+2016 dataset of 36.1fb^{-1} of 13 TeV data: the full analysis of this data will improve sensitivities still further and allow additional measurements to be performed. Furthermore, the ATLAS dataset should more than double in 2017, resulting in a dataset over four times as large as those used by the measurements reported here, with consequent increases in precision and reach.

References

[1] ATLAS Collaboration, *The ATLAS Experiment at the CERN Large Hadron Collider*, *JINST* **3** S08003 (2008).

[2] ATLAS Collaboration, *Observation of a new particle in the search for the Standard Model Higgs boson with the ATLAS detector at the LHC*, *Phys. Lett.* B**716**, 1 (2012).

[3] CMS Collaboration, *Observation of a new boson at a mass of 125 GeV with the CMS experiment at the LHC*, *Phys. Lett.* B**716**, 30 (2012).

[4] ATLAS Collaboration, ATLAS-CONF-2016-079, http://cds.cern.ch/record/2206253.

[5] ATLAS Collaboration, ATLAS-CONF-2016-067, http://cds.cern.ch/record/2206210.

[6] ATLAS Collaboration, ATLAS-CONF-2016-081, http://cds.cern.ch/record/2206272.

[7] D. de Florian et al.,*Handbook of LHC Higgs Cross Sections: 4. Deciphering the Nature of the Higgs Sector*, CERN Yellow Reports: Monographs Volume 2/2017 [hep-ph:1610.07922].

[8] ATLAS Collaboration, ATLAS-CONF-2016-112, http://cds.cern.ch/record/2231811.